

A control-oriented dynamic wind farm flow model: “WFSim”

S. Boersma¹, P.M.O. Gebraad², M. Vali³, B.M. Doekemeijer¹ and
J.W. van Wingerden¹

¹ Delft Center for Systems and Control, Delft University of Technology, The Netherlands

² Siemens Wind Power, Denmark

³ Wind Energy System Research Group, ForWind, University of Oldenburg, Germany

E-mail: S.Boersma@tudelft.nl

Abstract. In this paper, we present and extend the dynamic medium fidelity control-oriented Wind Farm Simulator (WFSim) model. WFSim resolves flow fields in wind farms in a horizontal, two dimensional plane. It is based on the spatially and temporally discretised two dimensional Navier-Stokes equations and the continuity equation and solves for a predefined grid and wind farm topology. The force on the flow field generated by turbines is modelled using actuator disk theory. Sparsity in system matrices is exploited in WFSim, which enables a relatively fast flow field computation. The extensions to WFSim we present in this paper are the inclusion of a wake redirection model, a turbulence model and a linearisation of the nonlinear WFSim model equations. The first is important because it allows us to carry out wake redirection control and simulate situations with an inflow that is misaligned with the rotor plane. The wake redirection model is validated against a theoretical wake centreline known from literature. The second extension makes WFSim more realistic because it accounts for wake recovery. The amount of recovery is validated using a high fidelity simulation model Simulator fOr Wind Farm Applications (SOWFA) for a two turbine test case. Finally, a linearisation is important since it allows the application of more standard analysis, observer and control techniques.

1. Introduction

It is beneficial to group turbines together in a so-called wind farm for several economic reasons, even though this results in additional challenges. By grouping turbines together, an interaction, via the wakes, will be established between upwind and downwind turbines. It is necessary to take these interactions into account when analysing and controlling the performance of a wind farm. Typical performance indicators are power production and load mitigation and can be influenced using wake redirection and axial induction control [1]. The objective is then to design controllers such that certain performance can be guaranteed for the complete wind farm. In order to design and test these controllers, there is a need for wind farm models. Several models exist ranging from high fidelity (*e.g.* SOWFA [2]) to medium fidelity (*e.g.* Dynamic Wake meandering Model [3] or FLOW Redirection and Induction Dynamics [4]) to parametric



models (*e.g.* Jensen [5] or FLOW Redirection and Induction in Steady-state (FLORIS) [6]), each with their own advantages and disadvantages. WFSim can be considered a medium fidelity flow model. It was first published in [7] after which it was transformed to a quasi linear parameter varying (LPV) system in [8]. The objective of WFSim is to approximate the 2D velocity flow vectors in a wind farm while it in addition can be used for controller design. The latter can be achieved by the (optional) transformation to a quasi-LPV model. Before the work presented here, WFSim did not have the option to do wake redirection control. Since recent studies have shown the potential of such a control strategy (see *e.g.* [9]), it is important to include this in WFSim. Also not present in WFSim is a turbulence model, which would account for wake recovery, an essential characteristic of a wake and hence crucial for improving the model. In this paper, both of these items will be included in WFSim. In addition, a linearisation will be developed so that WFSim will become more suitable for standard control design methods. Each improvement is subsequently described.

2. WindFarmSimulator

WFSim is based on the incompressible 2D Navier-Stokes momentum equations and conservation of mass equation which are defined in continuous time as:

$$\rho \frac{\partial u}{\partial t} + \rho \nabla \cdot u \mathbf{u} = -\frac{\partial p}{\partial x} + \mu \nabla \cdot \text{grad}(\mathbf{u}) + S^x + T^x, \quad (1)$$

$$\rho \frac{\partial v}{\partial t} + \rho \nabla \cdot v \mathbf{u} = -\frac{\partial p}{\partial y} + \mu \nabla \cdot \text{grad}(\mathbf{u}) + S^y, \quad (2)$$

$$0 = \rho \text{grad}(\mathbf{u}), \quad (3)$$

where $\rho = 1.2$ [kg/m³] is the air density, $\mu = 18 \cdot 10^{-5}$ [kg/m/s] the dynamic viscosity and the operators ∇ , grad , $\frac{\partial}{\partial t}$ are the divergence, gradient and partial derivative, respectively. Furthermore we have $\mathbf{u} = [u \ v]^T$ [m/s] being the velocity components in the x and y-direction and pressure p . The forces exerted by turbines on the flow are represented by S^x and S^y in the x and y-direction, respectively. The term T^x represents the contribution of the turbulent shear stresses to the momentum balance. It is assumed that the non-yawed turbine is oriented perpendicular to the dominant flow direction hence only turbulence in the x-momentum equation is included. Given that the above set of equations does not have an analytic solution for the boundary conditions and forcing terms which we will define later, spatially discretizing the set of equations is inevitable. In [8], the authors show that by using the Finite Volume Method (FVM) as presented in [10], defining the state variables u_k, v_k and p_k at time step k as:

$$u_k = \begin{pmatrix} u_{3,2} \\ \vdots \\ u_{3,N_y-1} \\ u_{4,2} \\ \vdots \\ u_{4,N_y-1} \\ \vdots \\ u_{N_x-1,2} \\ \vdots \\ u_{N_x-1,N_y-1} \end{pmatrix}, \quad v_k = \begin{pmatrix} v_{2,3} \\ \vdots \\ v_{2,N_y-1} \\ v_{3,3} \\ \vdots \\ v_{3,N_y-1} \\ \vdots \\ v_{N_x-1,3} \\ \vdots \\ v_{N_x-1,N_y-1} \end{pmatrix}, \quad p_k = \begin{pmatrix} p_{2,2} \\ \vdots \\ p_{2,N_y-1} \\ p_{3,2} \\ \vdots \\ p_{3,N_y-1} \\ \vdots \\ p_{N_x-1,2} \\ \vdots \\ p_{N_x-1,N_y-1} \end{pmatrix}, \quad (4)$$

and temporally discretizing the set of equations using the implicit method as also described in [10], the equations given in Eq.(1), Eq.(2) and Eq.(3) can be transformed to the following set of nonlinear algebraic difference equations:

$$\underbrace{\begin{pmatrix} A_x(u_k, v_k) & 0 & B_1 \\ 0 & A_y(u_k, v_k) & B_2 \\ B_1^T & B_2^T & 0 \end{pmatrix}}_{A(x_k)} \underbrace{\begin{pmatrix} u_{k+1} \\ v_{k+1} \\ p_{k+1} \end{pmatrix}}_{x_{k+1}} = \underbrace{\begin{pmatrix} b_1(u_k, v_k) \\ b_2(u_k, v_k) \\ b_3 \end{pmatrix}}_{b(x_k)}, \quad (5)$$

with $u_k \in \mathbb{R}^{n_u}$, $v_k \in \mathbb{R}^{n_v}$, $p_k \in \mathbb{R}^{n_p}$ the velocity vectors in the x-direction, y-direction and the pressure vector at time k , respectively. The constants N_x and N_y are the number of grid points in the x- and y-direction respectively. Each component of u_k , v_k and p_k represents a velocity and pressure respectively at a point in the field defined by the subscript. For more background information, the interested reader is referred to [8]. Here, the authors also show that the set of algebraic difference equations can be transformed to a nonlinear implicit system. In this paper we will however use the set of equations as defined in Eq.(5). Computational cost for solving this set of equations is reduced by exploiting sparsity and by applying the reverse Cuthill-McKee algorithm [11]. To clarify the meaning of vectors and equations given in Eq.(4) and Eq.(5) respectively, a grid example is depicted in Figure 1. Here we have $N_x = N_y = 5$ and a dominant flow indicated by the arrow. Non-yawed turbines are placed perpendicular to this dominant flow.

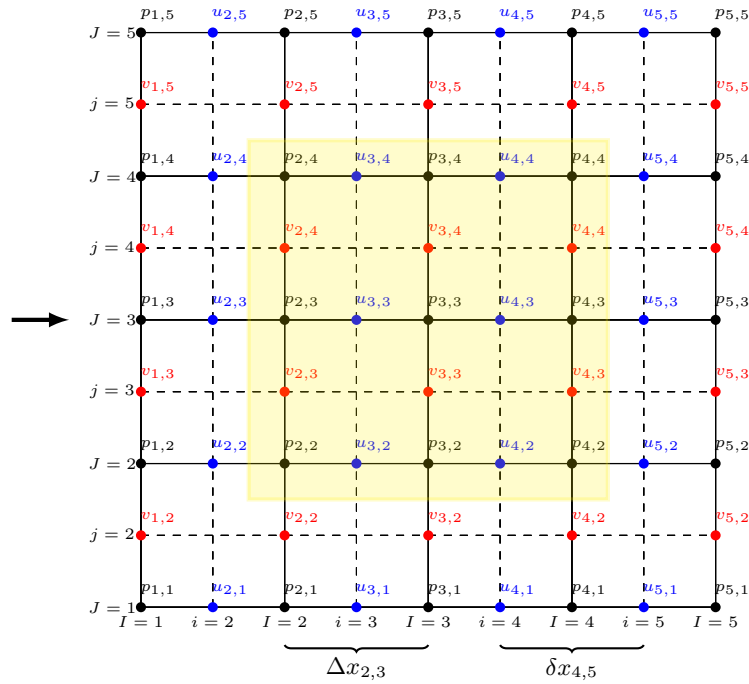


Figure 1: Example of a staggered grid.

In order to emphasize the contributions of this paper we first give b_1 and b_2 in the right hand side of Eq.(5):

$$b_1 = b_x + c_x u_k + S_k^x + T_k^x, \quad b_2 = b_y + c_y v_k + S_k^y. \quad (6)$$

The term b_3 only depends on spacing and boundary velocities. Furthermore, b_x and b_y are terms depending on boundary velocities and velocity components in the field and c_x and c_y only

depend on spacing. The boundary conditions will be given hereafter. WFSim allows us to carry out axial induction based control via the term S_k^x and wake redirection control via the term S_k^y if we follow the assumption given previously. We assumed that the non-yawed turbine is oriented perpendicular to the dominant flow direction (see Figure 1). Both terms S_k^x and S_k^y will be defined in this paper. The turbulence term T_k^x will also be defined and will result in wake recovery of the flow behind turbines. First however, the boundary and initial conditions will be defined.

Boundary conditions and initial conditions For the u and v velocity, we prescribe first order conditions on the west side of the grid. We note that the boundary conditions are related to the ambient inflow defined by u_b and v_b . We prescribe zero stress boundary conditions on the other boundaries. Therefore, for u and v we define:

$$\begin{aligned} u_{2,J} &= u_b & \text{for } J = 1, 2, \dots, N_y, & & v_{1,j} &= v_b & \text{for } j = 2, 2, \dots, N_y, \\ u_{i,N_y} &= u_{i,N_y-1} & \text{for } i = 3, 4, \dots, N_x, & & v_{I,N_y} &= v_{I,N_y-1} & \text{for } I = 2, 3, \dots, N_x, \\ u_{i,1} &= u_{i,2} & \text{for } i = 3, 4, \dots, N_x, & & v_{I,2} &= v_{I,3} & \text{for } I = 2, 3, \dots, N_x, \\ u_{N_x,J} &= u_{N_x-1,J} & \text{for } J = 2, 3, \dots, N_x - 1, & & v_{N_x,j} &= v_{N_x-1,j} & \text{for } j = 3, 4, \dots, N_y - 1, \end{aligned}$$

with N_x and N_y the number of grid points in the x- and y-direction respectively. For the initial conditions, we define all u and v velocity components in the field as u_b and v_b respectively, the boundary velocity components. The initial pressure field is set to zero which implies that it can be seen as a deviation variable from a nominal value. In the following section we will introduce expressions for the source terms S_k^x and S_k^y . Then we will introduce the turbulence term T_k^x .

2.1. Rotor model

In Figure 2 we illustrate a two dimensional schematic representation of a turbine with yaw angle γ and local wind direction at the turbine rotor defined by the angle ϕ .

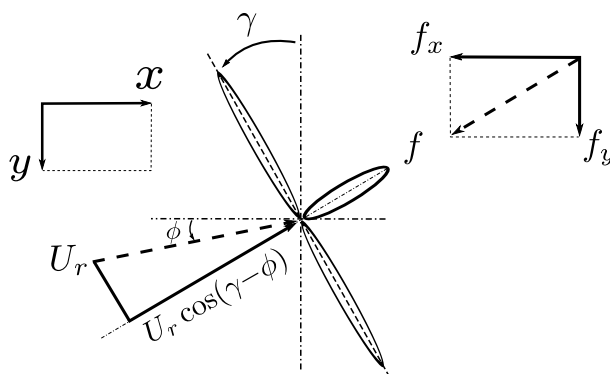


Figure 2: Schematic representation of a turbine with yaw angle γ , wind direction angle at the rotor ϕ and rotor velocity U_r . Figure taken and adapted from [12].

According to momentum theory, the following force term can be defined:

$$S_k = C_T \frac{1}{2} \rho A_r U_{\text{effect}}^2, \quad (7)$$

with thrust coefficient C_T , air density ρ , rotor upwind velocity U_{effect} and rotor swept area A_r which is a function of the rotor diameter D_r . In actuator disk theory, the thrust coefficient is defined as $C_T = 4a(1-a)$ with a the turbine's axial induction. However, the authors in [13] show that for high axial inductions, this thrust coefficient is not accurate with respect to measurements and a Glauert correction is introduced. The following adaptation of the C_T definition is proposed in [13]:

$$C_T(a) = \begin{cases} 4aF(1-a), & \text{if } 0 \leq a \leq 0.4 \\ \left(8/9 + (4F - 40/9)a + (50/9 - 4F)a^2\right) & \text{if } 0.4 < a < 1 \end{cases} \quad (8)$$

In this paper, we set $F = 1.75$. This does not only result in a relative increase of C_T for high axial inductions, but also for low axial inductions. Since U_{effect} is not well defined in a wind farm, it is interesting to write the force in terms of the rotor velocity. We define the following relations:

$$\beta = \frac{a}{1-a}, \quad U_{\text{effect}} = \frac{U_r \cos(\gamma - \phi)}{1-a}, \quad U_r = \sqrt{u_r^2 + v_r^2}, \quad (9)$$

with U_r the flow velocity vector at the rotor with direction defined by the angle ϕ and γ the yaw angle. Note that u_r and v_r are velocity components at the rotor in x- and y-direction respectively. Substituting these relations in Eq.(7) yields the following expression for the force S_k :

$$S_k = \frac{1}{2} \rho A_r C_T(\beta) [U_r \cos(\gamma - \phi)(\beta + 1)]^2. \quad (10)$$

Now we can define the force in the x- and y-direction as

$$S_k^x = -S_k \cos(\gamma), \quad S_k^y = S_k \sin(\gamma). \quad (11)$$

In the following section we will define the turbulence term T_k^x .

2.2. Turbulence model

The term T^x in Eq.(1) represents the mixing length turbulence model [14]. T^x can, after following the assumptions as presented in [15], be defined as:

$$T^x = \rho l_m \frac{\partial}{\partial y} \left[\left| \frac{\partial u}{\partial y} \right| \frac{\partial u}{\partial y} \right], \quad (12)$$

with parameter l_m which we found after tuning to be $l_m = 0.3D_r$ and D_r the rotor diameter. Spatially discretizing Eq.(12) using the FVM yields an expression for T_k^x . Since this term depends only on u velocity components other than the velocity components which occur in the vector b_1 , the expression for T_k^x can be absorbed in the matrix $A_x(u_k, v_k)$. To be more precise, the first row of Eq.(5) will then read as

$$\bar{A}_x(u_k, v_k)u_{k+1} + B_1 p_{k+1} = b_1. \quad (13)$$

The other rows in Eq.(5) will not change. In addition, the structure in $\bar{A}_x(u_k, v_k)$ will be equivalent to $A_x(u_k, v_k)$ as defined in Eq.(5) though only the magnitude of coefficients will change due to the additional turbulence term. The structure preserving property is an advantage of using the mixing length model since fast solving is retained.

2.3. Software implementation

In this section we present a pseudo code to illustrate how the solver computes flow fields u_{k+1}, v_{k+1} and p_{k+1} for a given input w_k representing the control signals β, γ for all turbines in the wind farm under consideration. Once initialized, the program enters a for-loop until final time $k = N$. In this for-loop, the program enters a while-loop until the flow field converges. Convergence can occur in two cases. First, when the maximum amount of iterations it_{max} is achieved and second, when the 2-norm of $x_{k+1} - x_k$ is smaller than a pre specified threshold ε . Note that by initialising $it_{max} = 1$, WFSim starts directly with the time for-loop without first converging to a steady state solution. Instead of computing a time depending solution, WFSim can also find a steady state solution. In this case, $N = 1$ and the sample time $h = \infty$.

Algorithm 1: Pseudo code for WFSim

```

1  $x_0 \leftarrow \text{InitialField}(u_b, v_b, p_b)$  % Compute initial flow fields
2  $w_0 \leftarrow \text{ControlVariable}(x_0)$  % Compute initial control signals
3  $h \leftarrow 1$  % Define sample period  $h$ 

4 if Steady state solution
5    $h \leftarrow \infty$ 
6    $N \leftarrow 1$ 
7 end

8 for  $k = 0 : N$  % Time for-loop until final time  $N$ 
9   while  $\delta > \varepsilon$  &  $it < it_{max}$ 
10     $[A(x_k), b(x_k)] \leftarrow \text{UpdateSetofEquations}(x_k, w_k, k, h)$ 
11     $x_{k+1} \leftarrow \text{FindSolution}(A(x_k), b(x_k))$ 
12     $\delta \leftarrow \|x_{k+1} - x_k\|_2$ 
13     $it \leftarrow it + 1$ 
14  end
15   $1 \leftarrow it_{max}$ 
16   $w_{k+1} \leftarrow \text{ControlVariable}(x_{k+1})$ 
17 end

```

2.4. Linearisation

WFSim is based on the nonlinear Navier-Stokes equations and the continuity equation. For these types of models, guarantees on stability, observability and controllability can not easily be ensured. However, when a linearised version is available, these measures can locally be defined around the point of linearisation. It is therefore interesting to also have a linearised version of WFSim available. Stability, observability and controllability can in this case be ensured for the linearisation point. When linearising Eq.(5), the following set of equations can be obtained:

$$\underbrace{\begin{pmatrix} A_1 & A_2 & B_1 \\ A_3 & A_4 & B_2 \\ B_1^T & B_2^T & 0 \end{pmatrix}}_{\delta A(\delta x_k)} \underbrace{\begin{pmatrix} \delta u_{k+1} \\ \delta v_{k+1} \\ \delta p_{k+1} \end{pmatrix}}_{\delta x_{k+1}} = \underbrace{\begin{pmatrix} b_4 \\ b_5 \\ b_6 \end{pmatrix}}_{\delta b(x_k)}, \quad (14)$$

with $\delta u_k \in \mathbb{R}^{n_u}$, $\delta v_k \in \mathbb{R}^{n_v}$, $\delta p_k \in \mathbb{R}^{n_p}$ the velocity vectors in x-direction, y-direction and the pressure terms at time k , respectively. Note that the states are deviation variables relative to

the point of linearisation. Due to the fact that the matrix $\delta A(\delta x_k)$ still contains B_1 and B_2 we can apply the method as presented in [8] so that Eq.(14) can be transformed to a linear descriptor model. This can, in turn, be used to compute a frequency response which is useful for analysis purposes.

3. Results

In this section we will compare WFSim with a theoretical wake centreline taken from [9] and with a spatially-averaged wake velocity profile obtained from SOWFA data. The first comparison is to assess if the wake redirection under a specified yaw angle γ is realistic. In order to evaluate whether the flow fields behind the turbines computed with WFSim are such that they can approximate spatially-averaged wake velocity profiles from a high-fidelity solver, the model outputs were compared to data obtained from SOWFA. Finally, we will present the Bode magnitude plot of a two turbine wind farm using the linearised model.

3.1. Yaw control variable validation

In this section we use a single turbine set up for validating the wake redirection model. Table 1 gives the important simulation parameters.

Table 1: Simulation parameters.

Parameter	Value [units]	Parameter	Value [units]
u_b	8 [m/s]	N	1 [-]
v_b	0 [m/s]	h	1 [s]
p_b	0 [Pa]	γ_1	35 [deg]
N_x	120 [-]	β_1	$\frac{1}{2}$ [-]
N_y	100 [-]	D_{r1}	90 [m]

With WFSim, a steady state flow field has been computed using an exponential grid. Note that in this particular case we have approximately $3.6 \cdot 10^4$ states. Figure 3 illustrates the steady state u -velocity. The middle black dotted line represents the theoretical wake centreline and the outer black dotted lines define a theoretical wake diameter also taken from [9]. The steady state solution was computed on a standard notebook in approximately 7.5 [s].

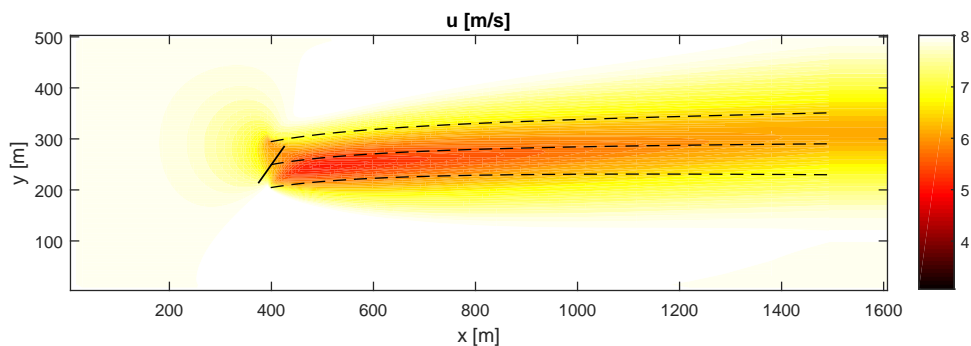


Figure 3: Steady state u -velocity for a single turbine set up with $\gamma_1 = 35$ [deg] and $\beta_1 = \frac{1}{2}$. The black dotted lines are the theoretical wake centreline and wake diameter taken from [9].

We can observe in Figure 3 that the simulation results are a good approximation of the theoretical centreline in steady state. This indicates that WFSim can potentially be used for wake redirection control.

3.2. Comparison with SOWFA

In this section we will compare WFSim with SOWFA data. We calculated spatially-averaged wake velocity profiles $U_c(t)$ by taking the velocity in the x-direction over the entire domain and averaging the velocities in the y-direction over the rotor diameter. In both models the same control signal excitation is applied to the turbines, and then the spatially-averaged profiles $U_c(t)$ are compared at different time instances.

A perfectly aligned two turbine wind farm starting from a fully uniform flow has been simulated in SOWFA and WFSim. The control signals for turbine 1 and 2, β_1 and β_2 , could be extracted from the SOWFA data with β_1 illustrated in Figure 4. The switching in this signal corresponds to the first turbine actuation: a pseudo random binary signal on the collective blade pitch angle. Again, an exponential grid is chosen and in this particular case we have approximately 15000 states. The other simulation parameters are given in Table 2.

Table 2: Simulation parameters.

Parameter	Value [units]	Parameter	Value [units]
u_b	8 [m/s]	N	2000 [-]
v_b	0 [m/s]	h	1 [s]
p_b	0 [Pa]	$\{\gamma_1, \gamma_2\}$	$\{0, 0\}$ [deg]
N_x	100 [-]	$\{\beta_1, \beta_2\}$	{Figure 4, 0.3} [-]
N_y	50 [-]	$\{D_{r1}, D_{r2}\}$	$\{126, 126\}$ [m]

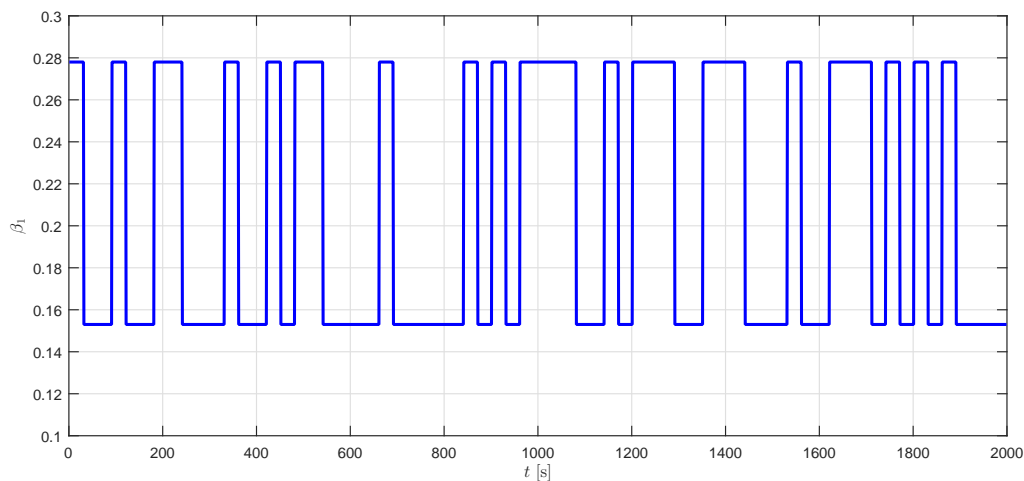


Figure 4: The control signal β_1 of the first turbine.

WFSim has computed a time depending solution where each time step computation took approximately 0.1 [s]. From the found u -flow field we compute the spatially-averaged wake

velocity profile $U_c(t)$. This and the spatially-averaged wake velocity profile extracted from SOWFA data are illustrated in Figure 5. Here it can be seen that WFSim is able to match SOWFA's $U_c(t)$ qualitatively well in the near wake region. The mixing length turbulence model included in WFSim introduces a desired wake recovery, but still underestimates the wake recovery with respect to SOWFA data in the far wake region. This is due to *i.a.* the relatively simple mixing length turbulence model while SOWFA contains a more advanced turbulence model. Furthermore, in SOWFA wake meandering and wake deflection due to direction of rotor rotation (see [16]) is also modelled. This implies that wakes are not symmetrically aligned behind the turbines in SOWFA.

This far wake region error can be minimised by using for example a Kalman estimator as has been illustrated in [17]. In Table 3, the variance accounted for (VAF) [18] is presented for different time instances. We note that it is desirable to have a high VAF since then, the spatially-averaged wake velocity profiles match the most.

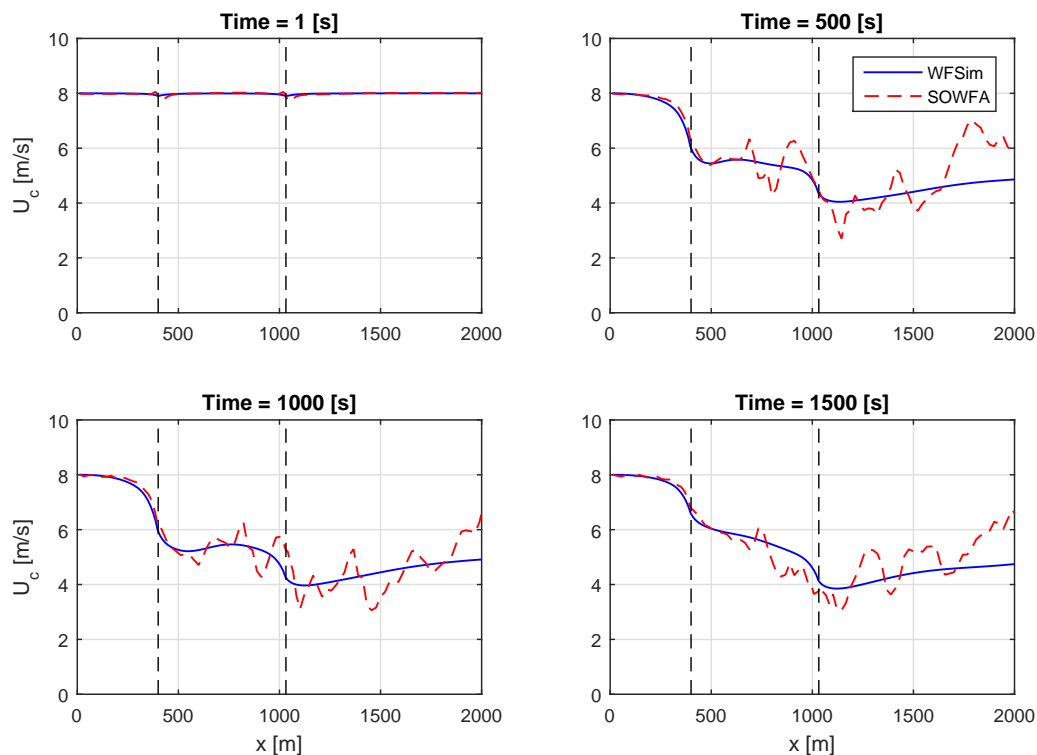


Figure 5: Spatially-averaged wake velocity profiles $U_c(t)$ obtained with WFSim (blue) and SOWFA, at different time instances t . The black dotted vertical lines represent the turbine positions.

Table 3: VAF [18] between spatially-averaged wake velocity profiles $U_c(t)$ obtained from SOWFA and WFSim data.

Time [s]	VAF (%)	Time [s]	VAF (%)
1	16.8	1000	82.1
500	73.5	1500	77.5

3.3. Frequency response

The linearisation is computed for the previously described two turbine case. Figure 6 depicts the amplitude frequency responses of the linearised model. Each plot is a response from the input β_i to a rotor velocity u_{r_i} for $i = 1, 2$. This is indicated as $T_{\beta_i \rightarrow u_{r_i}}$. We can clearly observe that the second input β_2 , the scaled axial induction of the second turbine, is not able to influence the rotor velocity at the first turbine u_{r_1} . We also see that the control input β_1 is able to influence both rotor velocities. These observations coincide perfectly with the physical system, the aligned two turbine wind farm and thus validate the linearised WFSim qualitatively.

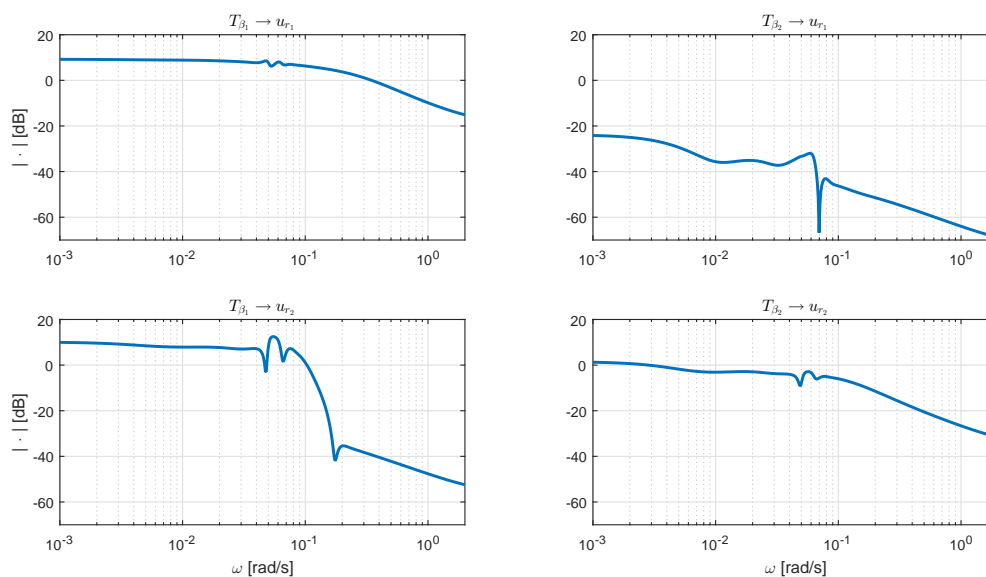


Figure 6: Amplitude frequency responses of the linearised model in steady-state.

4. Conclusion

In this paper we have shown that, including the extensions presented in this paper, WFSim is a candidate control-oriented dynamic flow model. The wake redirection model and turbulence model were tested and results illustrate, for a two turbine case, similar behaviour with respect to SOWFA data. Further model validation for different flow fields, farm topologies etc. is necessary and ongoing. In addition, the wake redirection model will be validated against dynamical simulation results instead of, as presented in this paper, a steady state flow field. Further quantitative validation/analysis of linearised model is also ongoing. A subsequent step is designing a controller using WFSim such that certain performance can be ensured. Then, this controller can be tested on SOWFA or even better, a real wind farm.

References

- [1] T. Knudsen, T. Bak, and M. Svenstrup, "Survey of wind farm control power and fatigue optimization," *Wind Energy*, 2014.
- [2] M. Churchfield, S. Lee, J. Michalakes, and P. J. Moriarty, "A numerical study of the effects of atmospheric and wake turbulence on wind turbine dynamics," *Journal of Turbulence*, 2012.
- [3] G. Larsen, H. Madsen, F. Bingl, J. Mann, S. Ott, J. Srensen, V. Okulov, N. Troldborg, M. Nielsen, K. Thomsen, T. Larsen, and R. Mikkelsen, "Dynamic wake meandering modelling," tech. rep., Ris National Laboratory, 2007, 2007.
- [4] P. M. O. Gebraad and J. W. van Wingerden, "A control-oriented dynamic model for wakes in wind plants," *TORQUE*, 2014.
- [5] N. O. Jensen, "A note on wind generator interaction," 2005.
- [6] P. M. O. Gebraad, F. W. Teeuwisse, J. W. van Wingerden, P. A. Fleming, S. D. Ruben, J. R. Marden, and L. Y. Pao, "A data-driven model for wind plant power optimization by yaw control," *American Control Conference*, 2014.
- [7] P. Torres, J. W. van Wingerden, and M. Verhaegen, "Modeling of the flow in wind farms for total power optimization," *Control and Automation*, 2011.
- [8] S. Boersma, J. W. van Wingerden, M. Vali, and M. Kühn, "Quasi linear parameter varying modeling for wind farm control using the 2D Navier Stokes equations," *American Control Conference*, 2016.
- [9] P. M. O. Gebraad, F. W. Teeuwisse, J. W. van Wingerden, P. A. Fleming, S. D. Ruben, J. R. Marden, and L. Y. Pao, "Wind plant power optimization through yaw control using a parametric model for wake effects - a CFD simulation study," *Wind Energy*, 2014.
- [10] H. K. Versteeg and W. Malalasekera, "An introduction to computational fluid dynamics: The finite volume method," 2007.
- [11] A. George and J. Liu, *Computer Solution of Large Sparse Positive Definite*. Prentice Hall, 1981.
- [12] Á. Jiménez, A. Crespo, and E. Migoya, "Application of a LES technique to characterize the wake deflection of a wind turbine in yaw," *Wind Energy*, 2010.
- [13] J. Marshall, L. Buhl, "A new empirical relationship between thrust coefficient and induction factor for the turbulent windmill state," tech. rep., National Renewable Energy Laboratory, 2005.
- [14] L. Prandtl, "Bericht über Untersuchungen zur ausgebildeten Turbulenz," 1925.
- [15] I. B. Celik, *Introductory Turbulence Modeling*. West Virginia University, 1999.
- [16] P. A. Fleming, P. M. O. Gebraad, S. Lee, J. W. van Wingerden, K. Johnson, M. Churchfield, J. Michalakes, P. Spalart, and P. Moriarty, "Evaluating techniques for redirecting turbine wakes using sowfa," *Renewable Energy*, vol. 70, pp. 211218, 2014.
- [17] B. M. Doekemeijer, J. W. van Wingerden, S. Boersma, and L. Y. Pao, "Enhanced Kalman filtering for a 2D CFD NS wind farm flow model," *TORQUE*, 2016.
- [18] M. Verhaegen and V. Verdult, *Filtering and System Identification: A Least Squares Approach*. Cambridge University Press, 1st ed., 2007.